Effect of the structure and charge of Au_{10} clusters on adsorption of hydrocarbons

D. A. Pichugina,[a,b] S. N. Lanin,[a] N. V. Kovaleva,[a] K. S. Lanina,[a] A. F. Shestakov,[b] and N. E. Kuz´menko[a]*

[a]Department of Chemistry, M. V. Lomonosov Moscow State University, Building 3, 1 Leninskie Gory, 119991 Moscow, Russian Federation. Fax: +7 (495) 932 8568. E-mail: daria@phys.chem.msu.ru
[b]Institute of Problems of Chemical Physics, Russian Academy of Sciences, 1 prosp. Akad. Semenova, 142432 Chernogolovka, Moscow Region, Russian Federation. Fax: +7 (496) 515 5420

The interaction of gold clusters Au_{10} of different structural and charge states with various hydrocarbons was studied by the PBE density functional method. Saturated hydrocarbons interact weakly with the neutral cluster Au_{10}, for charged Au_{10}^+ the alkane—cluster bond energies increase threefold. Unsaturated hydrocarbons interact with cluster surface more strongly than saturated hydrocarbons, while coordination to the benzene ring is possible for aromatic compounds PhC_2H, PhC_2H_3, and PhC_2H_5. The low-coordinative gold atoms located on the peaks and edges of the cluster are the active adsorption site of the cluster. The appearance of a positive charge on the cluster leads to a greater increase in the hydrocarbon—gold cluster bond energy than the transition from the planar 2D structure to the three-dimensional (3D) structure of the neutral cluster.

Key words: hydrocarbon, adsorption, gold, cluster, quantum chemistry, density functional theory.

The study of activation and adsorption of hydrocarbons on gold nanoclusters is important both from scientific and practical points of view. This is related first to the catalytic activity of gold nanoparticles in hydrocarbon oxidation, hydrogenation, and isomerization.[1] An interesting problem is the development and improvement of theoretical models for the detailed description and simulation of adsorption of hydrocarbons on the surface of the gold clusters.

The catalytic and adsorption properties of gold nanoparticles are determined by their structure, size, and charge.[2] Small gold clusters Au_n containing up to ten atoms are planar,[3] and their energy range is small. However, these clusters form many isomers with different structures. For example, more than six structures are known for Au_{10}, among which the planar 2D configuration is most stable (Fig. 1). The 3D structure of Au_{10} is characterized by a higher energy.[4] The interaction of the cluster with the support can change the planar form of the cluster and affect the electron density distribution.[5] Therefore, charged clusters and, first of all, cationic clusters Au_n^+ can be considered as models of gold nanoparticles.

Although the study of adsorption and activation of hydrocarbons on the gold clusters is urgent, this problem is insufficiently considered in the literature. It is known that molecules of saturated hydrocarbons interact very weakly

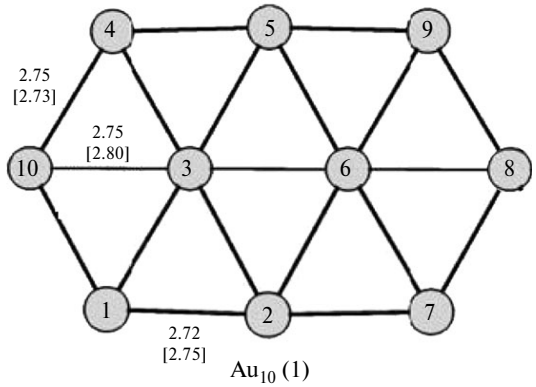

Fig. 1. Optimized structures of the Au_{10} clusters with different structures and charges. The distances Au—Au (Å) are presented for the neutral and charged (in brackets) clusters.

Published in Russian in *Izvestiya Akademii Nauk. Seriya Khimicheskaya,* No. 11, pp. 1987—1993, November, 2010.
1066-5285/10/5911-2039

with the gold surface. The energy of physical adsorption of *n*-alkanes on the Au(111) surface increases linearly with the chain length from 14.5 kJ mol^{-1} for methane to 93.6 kJ mol^{-1} for dodecane.[6] The interaction of *n*-alkanes with the tetrahedral cluster Au_{20} affords stable surface complexes, and the coordination sites of alkanes are the peaks and edges of the cluster, while their localization on the faces seems less probable.[7]

Adsorption of *n*-alkenes on the gold clusters is accompanied by the formation of complexes with different types of binding. In the bonds of the π-type the C atoms are coordinated to one metal atom, while in the bonds of the di-σ-type each C atom is bonded to different metal atoms.[8—11] The theoretical simulation of C_3H_6 adsorption on the Au_n clusters (n = 1—5, 8) showed that the bond energy depends on the structure of the cluster: the maximum value was obtained for Au_3 (122.5 kJ mol^{-1}), and the minimum value was obtained for the isolated atom (36.7 kJ mol^{-1}).[10] The energy of the C_3H_6—Au_n bond decreases on going from isolated clusters to the metal surface. Almost no adsorption of C_3H_6 occurs on the smooth Au(111) surface (E_{ad} = 6.7 kJ mol^{-1}), whereas on the model defective surface of Au/Au(111) the C_3H_6—Au_n bond energy increases to 61.8 kJ mol^{-1}. Thus, bonds formed by adsorption of unsaturated hydrocarbon on the cluster surface depends on its structure. However, it remains unclear whether effect of the cluster structure on the adsorption properties is stronger than the effect of the cluster charge.

This report is a continuation of the cycle of works devoted to the adsorption ability of the gold clusters.[7,12,13] We present the results of the systematic study of the adsorption and activation of hydrocarbons of various structure on the gold clusters, the nature of adsorption sites, and the influence of the structure and charge state of the cluster on its adsorption ability. The purpose of the present work is the quantum chemical simulation of adsorption of saturated and unsaturated hydrocarbons of various composition and structure on gold nanoparticles. The planar and 3D clusters Au_{10} and Au_{10}^+ are considered as models of particles. The established regularities of the influence of the hydrocarbon structure on its adsorption ability were compared with the results of gas-chromatographic studies of the composite Au(0.7%)/Al_2O_3.

Experimental

Quantum chemical simulation of the interaction of hydrocarbons with the gold clusters was performed by the density function theory (DFT) with the PBE (Perdew—Burke—Ernzerhow) nonempirical local functional.[14] The method chosen for calculation rather well reproduces the structure and energy properties of small-atomic gold-containing molecules and ions[15] and gives quite reliable results for the gold complexes and clusters.[13,16] The calculations were performed by the PRIRODA program.[17]

The relativistic effects for the gold atom are anomalously high.[18] In the framework of the non-relativistic approach, the use of the pseudo-potential makes it possible to efficiently take into account the most important scalar relativistic effects. For this purpose, we used the SBK pseudo-potential[19] for which the external electronic shells are described by the following sets of basic functions: H [311/1], C [311/311/11], and Au [51111/51111/5111]. Using the Gaussian 03 v. 01 program (see Ref. 20), we calculated the superposition error of the basis set used: it was less than 1 kJ mol^{-1} for all complexes. The contribution of the zero-point vibration energy to the total energy of the system was calculated in the harmonic approximation.

The type of stationary points of the potential energy surface (PES) was determined from analysis of the Hesse matrices and analytical calculation of the second derivatives. The adsorption energy E_{ad} of hydrocarbon C_xH_y on the gold cluster Au_n was calculated by the formula

$$E_{ad} = E(Au_n) + E(C_xH_y) - E(Au_nC_xH_y), \quad (1)$$

where $E(Au_nC_xH_y)$ is the energy of the optimized complex Au_n—hydrocarbon, and $E(Au_n)$ and $E(C_xH_y)$ are the energies of the optimized isolated cluster and hydrocarbon, respectively. In all cases, singlet states were considered for neutral systems, while doublet states were considered for charged systems, because the triplet and quintet states for the gold clusters are characterized by considerably higher energies (> 1 eV).[4]

The adsorption properties of the composite Au(0.7%)/Al_2O_3 were studied by gas chromatography. Measurements of the thermodynamic characteristics of adsorption at small and moderate coverages of the surface were performed on a Kristall 4000M chromatograph with a heat-conductivity detector (katharometer) using helium as a carrier gas. Glass chromatographic columns 25×0.2 cm in size were maintained at a constant temperature of 70—120 °C. Test compounds were normal hexane (n-C_6H_{14}), hexene (n-C_6H_{12}), and hexyne (n-C_6H_{10}), as well as benzene derivatives: ethylbenzene (PhC_2H_5), styrene (PhC_2H_3), and phenylacetylene (PhC_2H). A liquid 2-μL sample of the sorbate was injected into the chromatograph with a microsyringe. Chromatographic data were processed by the NetChrom V2.0 program. The specific retention volumes $V_{R,g}$ were calculated from the retention times measured at different temperatures. The adsorption heats Q were determined with allowance for the temperature dependence of the retention volume

$$\ln V_{R,g} = Q/(RT) + B, \quad (2)$$

where B is the integration constant. The error in determing the heat of adsorption is ±1 kJ mol^{-1}.

Results and Discussion

Interaction of hydrocarbons C_6 with Au_{10} and Au_{10}^+. The planar clusters Au_{10} and Au_{10}^+ (see Fig. 1) that mimic the Au(111) surface are formed by atoms of four types differed in the coordination number (CN)

Atom	Coordination number
3, 6	6
2, 5	4
1, 4, 7, 8, 9, 10	3

Hydrocarbon can coordinate to each of these atoms. The corresponding adsorption energies of hydro-

Table 1. Calculated energies of the complexes C_6H_{12}—Au_{10}, C_6H_{10}—Au_{10}, C_6H_{12}—Au_{10}^+, and C_6H_{10}—Au_{10}^+ relative to the energy of the complex with the coordination of hydrocarbon to atom 1 for planar Au_{10} and 7 for the bulk cluster Au_{10} (ΔE_0/kJ mol^{-1}) and the adsorption energy calculated for the most stable isomer by formula (1) (E_{ad}/kJ mol^{-1})

C_xH_y	Cluster	ΔE_0 for different types of binding (numbers of Au atom)					E_{ad}
		1	2	3	7	10	
C_6H_{10}	Au_{10}—1	0	21	65	—	1	76
	Au_{10}^+—1	0	34	36	—	–2	148
	Au_{10}—2	28	—	23	0	8	86
	Au_{10}^+—2	–1	—	–3	0	6	146
C_6H_{12}	Au_{10}—1	0	19	62	—	1	79
	Au_{10}^+—1	0	43	47	—	7	187
	Au_{10}—2	24	—	6	0	10	85
	Au_{10}^+—2	4	—	1	0	5	98

carbons C_6 calculated by formula (1) are listed in Table 1.

According to the previous theoretical studies,[7] saturated hydrocarbons (n-C_6H_{14}) are coordinated to the edge of the tetrahedral Au_{20} cluster with the bond energy 11 kJ mol^{-1}. The optimization of the structure of the C_6H_{14}—Au_{10} complex in which the interaction occurs with allowance for three contacts H—Au (Fig. 2) showed that the value of E_{ad} of n-C_6H_{14} on Au_{10} increased to 26 kJ mol^{-1}. On going to the charged planar cluster Au_{10}^+, E_{ad} increases almost three times and becomes equal to 74 kJ mol^{-1}.

Unsaturated hydrocarbons (n-C_6H_{12} and n-C_6H_{10}) interact with the gold cluster through the formation of a π-complex. The structures of the neutral and positively charged complexes C_6H_{12}—Au_{10} and C_6H_{10}—Au_{10} with different coordination of hydrocarbon relative to atoms 1, 2, 3, and 10 were optimized (see Fig. 2). The calculated total energies of each complex relative to the energy of the

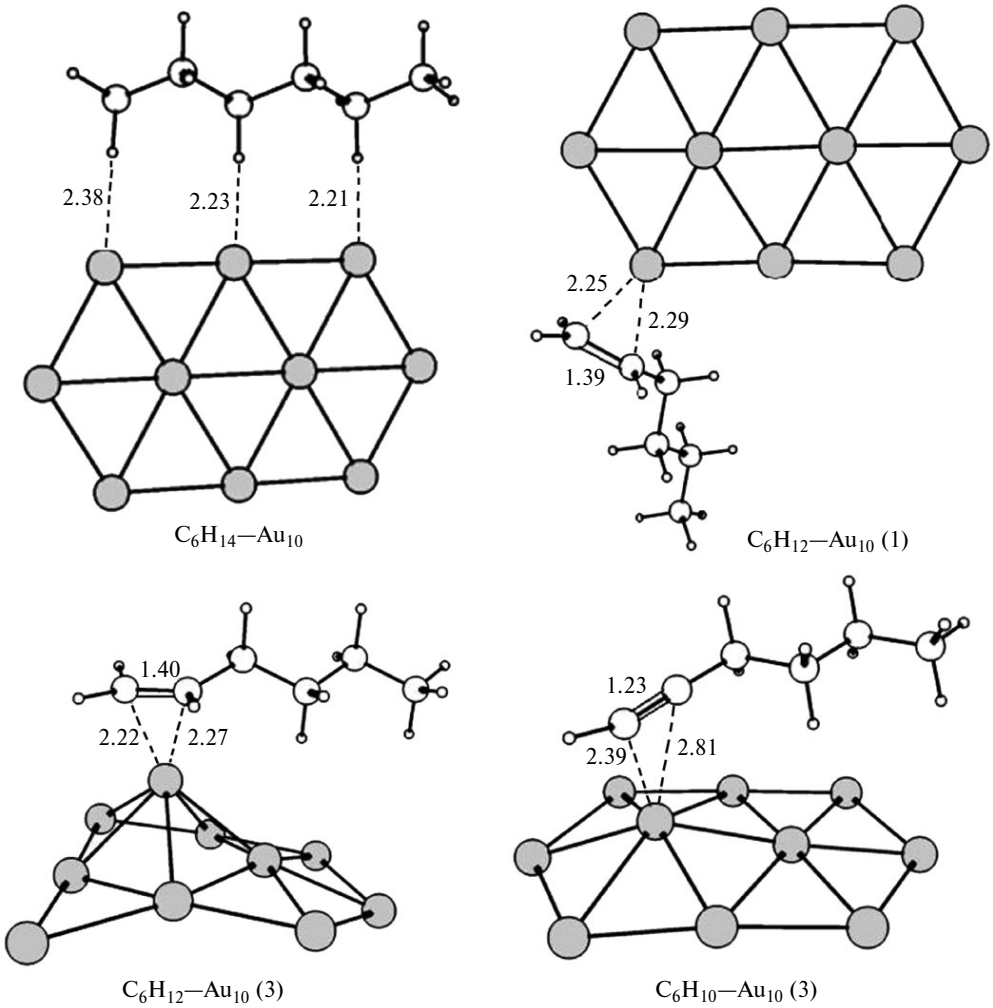

C_6H_{14}—Au_{10} C_6H_{12}—Au_{10} (1)

C_6H_{12}—Au_{10} (3) C_6H_{10}—Au_{10} (3)

Fig. 2. Optimized structures of the complexes of the planar Au_{10} cluster with C_6H_{14}, C_6H_{12}, and C_6H_{10} of different coordination modes of hydrocarbon to atoms 1, 2, and 3 (the atom number in the title of the complex is indicated in parentheses). Hereinafter in Figs 3, 6, and 8 the Au atoms are designated with gray and the C atoms are white; and the calculated distances are given in Å.

most stable isomer are listed in Table 1. The coordination of hydrocarbon to atoms 1 and 10 is most favorable for the neutral cluster, whereas the coordination to atom 2 is 20 kJ mol^{-1} less favorable. Alkenes and alkynes are bound to neutral planar Au_{10} with nearly the same E_{ad} equal to 76 and 79 kJ mol^{-1} for *n*-C_6H_{10} and *n*-C_6H_{12}, respectively. When hydrocarbon is coordinated to atom 3, the distortion of the cluster structure is possible (see Fig. 2), which is observed in the case of *n*-C_6H_{12}.

On going to the positively charged cluster Au_{10}^+, one can notice equalization of the values of relative energy of the complexes obtained by coordination to atoms 2 and 3. In this case, the adsorption energy of *n*-C_6H_{10} (148 kJ mol^{-1}) is considerably lower than that for *n*-C_6H_{12} (187 kJ mol^{-1}). The structures of the complexes are similar to those obtained earlier for the neutral cluster.

The following groups of nonequivalent atoms can be distinguished in the 3D Au_{10} cluster: 1 and 6 (CN = 5); 3, 4, 8, and 9 (CN = 4); 2, 7, 5, and 10 (CN = 3). According to the calculated data, among these atoms atom 7 has the highest adsorption strength. The adsorption energy of *n*-C_6H_{14} on 3D Au_{10} is lower than that on the planar one, E_{ad} = 18 kJ mol^{-1}. This is related, most likely, to a decrease in the number of H—Au contacts to two (Fig. 3). The optimized structures of complexes of *n*-C_6H_{10} and *n*-C_6H_{12} with 3D Au_{10} are shown in Fig. 3. It follows from Table 1 that the formation of complexes in which hydrocarbon is coordinated to atoms 7 and 10 is most favorable, and weaker binding is observed for atoms 1 and 3. On going from the two-dimensional to three-dimensional model, the energy of the hydrocarbon—cluster bond increases by 10 kJ mol^{-1} on the average for the both hydrocarbons. The values of E_{ad} for *n*-C_6H_{10} and *n*-C_6H_{12} are 86 and 85 kJ mol^{-1}, respectively. Thus, no selective adsorption of hydrocarbons containing double and triple bonds occurs on Au_{10} (3D).

The positive charge on the 3D cluster results in equalization of the energy of the complexes with different coordination modes of hydrocarbon and in an increase in E_{ad} compared to neutral 3D Au_{10}, and for *n*-C_6H_{10} the increase is more substantial (1.7 times). According to the calculation, selective adsorption of alkenes and alkynes is possible on 3D Au_{10}^+. Unlike the planar cluster Au_{10}^+, the 3D cluster more strongly adsorbs hydrocarbons containing the triple bond rather than those with the double bond. It was of interest to confirm experimentally the result obtained.

Measurement of the adsorption heat of hydrocarbons on the gold nanoparticles supported on alumina. The measurements of retention volumes of *n*-C_6H_{14}, *n*-C_6H_{12}, and *n*-C_6H_{10} on the composite Au(0.07%)/Al_2O_3 in the temperature range from 100 to 150 °C (Fig. 4) showed that the interaction of *n*-C_6H_{14} with the sample surface is weakest. At all temperatures the retention volumes increase on going from *n*-alkanes to *n*-alkenes and further to *n*-alkynes

$$V_m(C_6H_{14}) < V_m(C_6H_{12}) < V_m(C_6H_{10}).$$

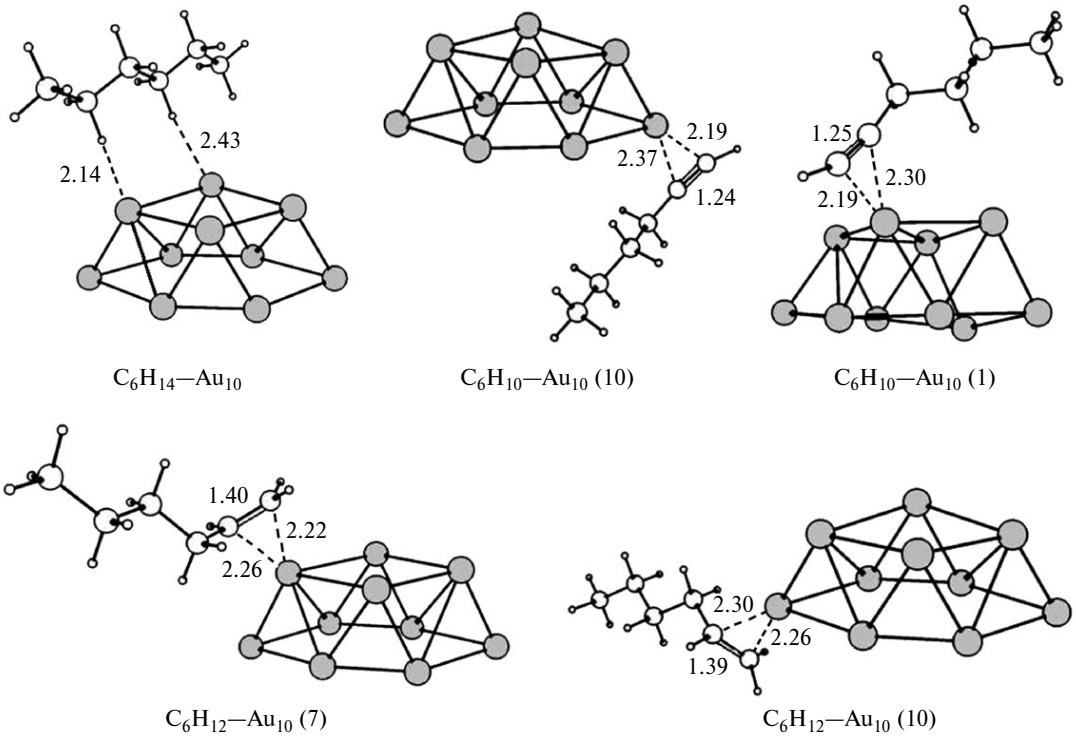

C_6H_{14}—Au_{10} C_6H_{10}—Au_{10} (10) C_6H_{10}—Au_{10} (1)

C_6H_{12}—Au_{10} (7) C_6H_{12}—Au_{10} (10)

Fig. 3. Optimized structures of the complexes of the bulk Au_{10} cluster with C_6H_{14}, C_6H_{12}, and C_6H_{10} with different coordination modes of hydrocarbons to atoms 1, 7, and 10.

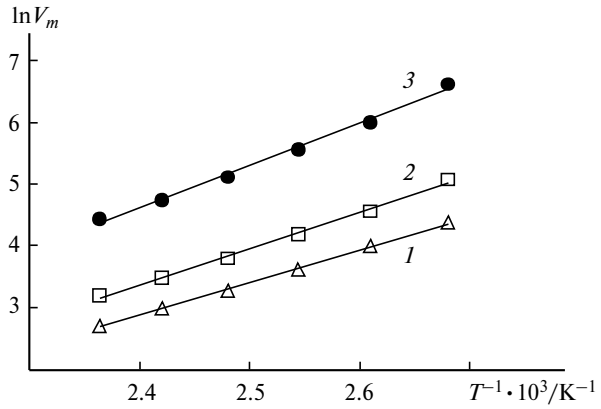

Fig. 4. Logarithm of the retention volume ($\ln V_m$) of n-C_6H_{14} (*1*), n-C_6H_{12} (*2*), and n-C_6H_{10} (*3*) *vs* inverse temperature for Au(0.07%)/Al_2O_3.

The calculation of the selectivity of adsorption α (ratio of retention volumes of adsorbates at different temperatures) revealed that the minimum selectivity is observed for the pair n-C_6H_{12}/n-C_6H_{14} the maximum one is observed for the pair C_6H_{10}/C_6H_{14} (Fig. 5, *a*), and the selectivity of adsorption of C_6H_{10}/C_6H_{12} is intermediate (Fig. 5, *b*). Thus, the Au(0.07%)/Al_2O_3 sample has a high selectivity of retention toward the studied aliphatic hydrocarbons. This tendency is confirmed by the quantum chemical simulation of hydrocarbons C_6 with Au_{10} in the case of the 3D charged gold cluster. This suggests that the model clusters considered adequately reflect the adsorption sites of the composite Au(0.07%)/Al_2O_3.

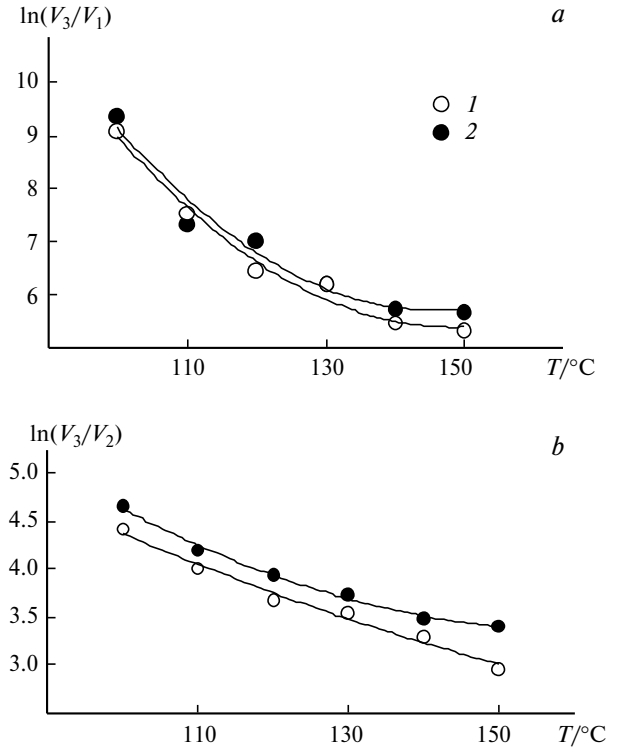

Fig. 5. Selectivity α *vs* temperature at $V_3/V_1 = C_6H_{10}/C_6H_{14}$ (*a*) and $V_3/V_2 = C_6H_{10}/C_6H_{12}$ (*b*): Au(0.7%)/Al_2O_3 (*1*) and Al_2O_3 (*2*).

The differential heats of adsorption (Q_v) determined by Eq. (2) increase on going from saturated hydrocarbons (45 kJ mol^{-1} for n-C_6H_{14} and 49 kJ mol^{-1} for n-C_6H_{12}) to unsaturated hydrocarbons (58 kJ mol^{-1} for n-C_6H_{10}). Similar dependence is probably related to both dispersion interactions and specific interactions of π-electron bonds with the active sites on the adsorbent surface. When Au particles are immobilized on the Al_2O_3 surface, the influence of the electron configuration of the carbon atoms on adsorption is retained. As with the starting γ-Al_2O_3, on going from *n*-alkane to *n*-alkene and then to *n*-alkyne with the equal number of atoms, the retention values on the composites (Au/Al_2O_3) increase due to the π-bonds.

Adsorption of light and aromatic hydrocarbons on the gold clusters. To determine the influence of the hydrocarbon structure on the adsorption energy on the cluster surface, we performed the quantum chemical simulation of the interaction of the planar and 3D clusters Au_{10} and Au_{10}^+ with simplest hydrocarbons C_2 (C_2H_6, C_2H_4, and C_2H_2) and with aromatic hydrocarbons Ph—C_2 (PhC_2H_5, PhC_2H_3, and PhC_2H). We considered the coordination only to the gold atom, which showed that highest activity in forming bonds with hydrocarbon C_6: this is atom 1 in planar Au_{10} and atom 7 in 3D Au_{10}. The optimized structures of the uncharged complexes Au_{10}—C_2H_x (x = 2, 4, 6) are presented in Fig. 6. Analogous structures of the hydrocarbon—cluster complexes with a slight change in the distances Au—C (2.20 Å for C_2H_2, 2.24 Å for C_2H_4) and Au—H (1.98 Å for C_2H_6) are formed for Au_{10}^+.

It seems interesting to compare the calculated values of E_{ad} for C_2H_6, C_2H_4, and C_2H_2 with the earlier obtained values for n-C_6H_{14}, n-C_6H_{12}, and n-C_6H_{10} (see Table 1). The dependences of the adsorption energy on the type of hydrocarbon for the planar and 3D clusters Au_{10} and Au_{10}^+ are shown in Fig. 7. It is seen that saturated hydrocarbons are bound most weakly to the gold cluster: their bond energy increases from 9 kJ mol^{-1} to 74 kJ mol^{-1} (C_6H_{14}, 2D). As it was expected, the energy of interaction increases with the chain length. In this case, the higher bond energy is characteristic of adsorption on the planar charged cluster. Similar regularity is observed for unsaturated hydrocarbons: the adsorption energy increases on going from hydrocarbons C_2 to C_6. Among the neutral clusters, the 3D cluster is the most active, while the planar cluster is the most active among the positively charged clusters. Ethylene is adsorbed more strongly than acetylene (the values of E_{ad} for C_2H_4 are 79 (2D cluster), 119 ($2D^+$ cluster), 70 (3D cluster), and 117 kJ mol^{-1} ($3D^+$ cluster)).

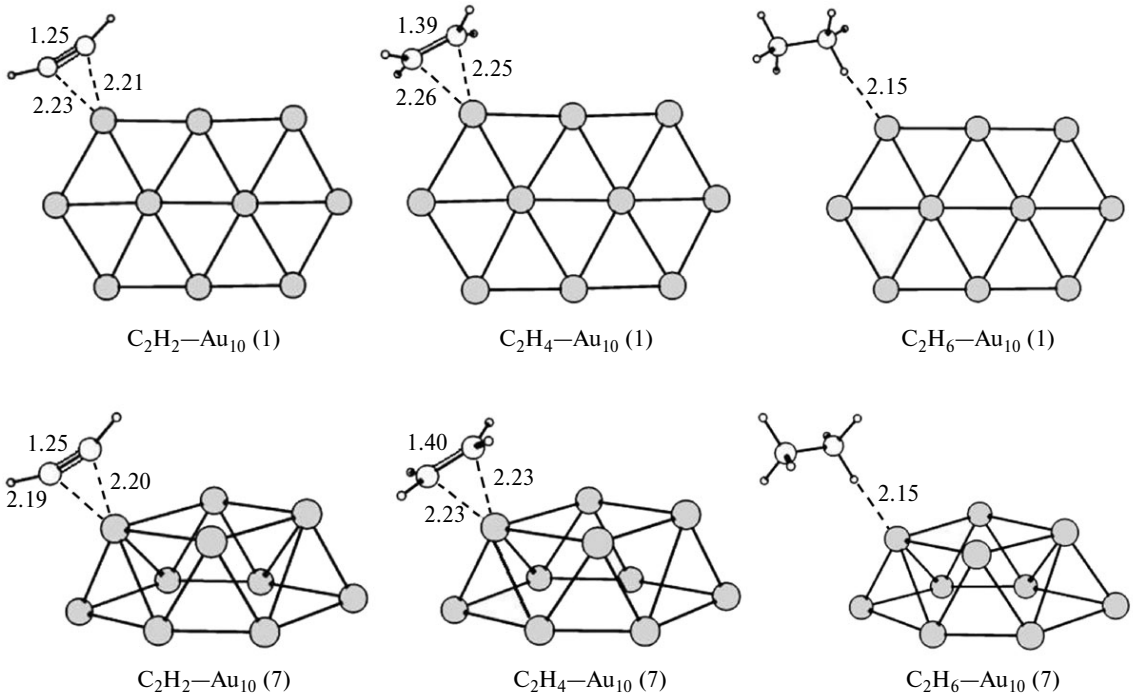

Fig. 6. Optimized structures of the neutral complexes of the planar and 3D Au_{10} clusters with C_2H_2, C_2H_4, and C_2H_6.

Aromatic compounds PhC_2H_5, PhC_2H_3, and PhC_2H can interact with the gold clusters not only through the formation of the π-complex with the substituent but also *via* the interaction with the aromatic system of the benzene ring (Fig. 8). In this case, the values of E_{ad} increase, for instance, for phenylethane E_{ad} increases to 31 E_{ad} kJ mol^{-1} ($2D^+$). The calculated bond energies of the 3D neutral gold cluster with PhC_2H (78 kJ mol^{-1}) and PhC_2H_3 (80 kJ mol^{-1}) coincide with the measured values of heats of adsorption of phenylacetylene (78 kJ mol^{-1}) and phenylethylene (74 kJ mol^{-1}) on the composites $Au(0.07\%)/Al_2O_3$.

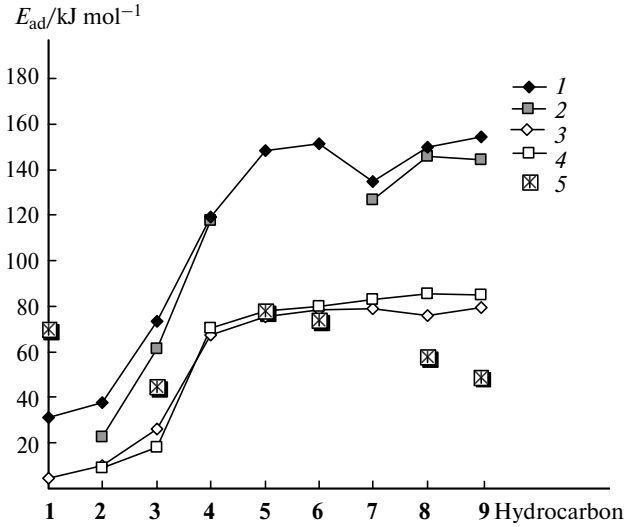

Fig. 7. Calculated (*1*—*4*) and experimental (*5*) adsorption energies of hydrocarbons PhC_2H_5 (**1**), C_2H_6 (**2**), C_6H_{14} (**3**), C_2H_2 (**4**), PhC_2H (**5**), PhC_2H_3 (**6**), C_2H_4 (**7**), C_6H_{10} (**8**), and C_6H_{12} (**9**) on the planar or 3D clusters Au_{10} and Au_{10}^+: planar cluster Au_{10}^+ (*1*), 3D cluster Au_{10}^+ (*2*), planar cluster Au_{10} (*3*), and 3D cluster Au_{10} (*4*); experimental value of adsorption heat on the composite $Au(0.7\%)/Al_2O_3$ (*5*).

The composites $Au(0.07\%)/Al_2O_3$ studied in the present work can be used as selective sorbents and catalysts of various reactions, including those involving hydrocarbons.[21] According to the performed simulation, the most probable adsorption and catalytic centers are $Au^{\delta+}$ ($0 < \delta < 1$), which can appear on the surface due to the interaction of a particle with the support or with the fragments of organic molecules remaining on the surface at some methods of production.[22] The use of supports containing surface Brönsted and/or Lewis acid sites favors an increase in these centers.[23] The introduction of an additional metal also affects the charge redistribution on the particle surface.[21]

Thus, the models developed for the adsorption of hydrocarbons of various composition and structure on the gold surface showed that the active adsorption sites are the most coordinatively unsaturated gold atoms situated on the peaks and edges of the cluster. If the cluster contains positively charged atoms, the energy of the hydrocarbon—cluster bond increases more considerably than for the distortion of the planar 2D structure. The comparison of the obtained theoretical results of the data of gas-chromatographic studies of $Au(0.7\%)/Al_2O_3$ showed that the con-

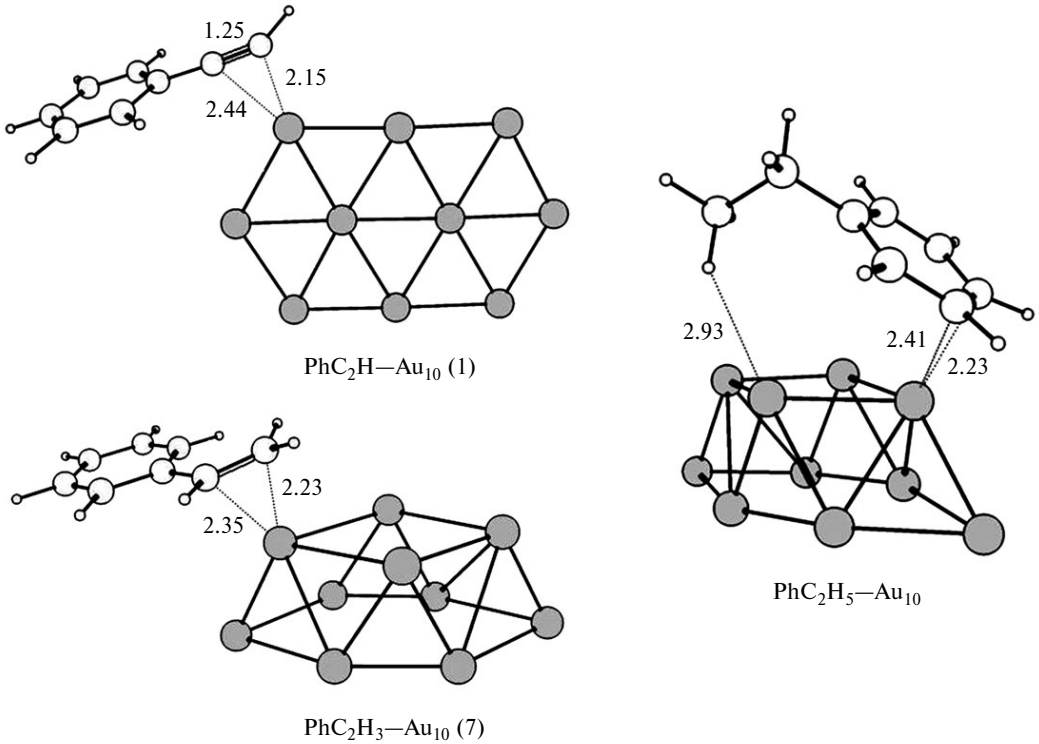

Fig. 8. Optimized structures of the neutral complexes of the planar and 3D clusters Au_{10} with PhC_2H, PhC_2H_3, and PhC_2H_5.

sidered model clusters adequately reflect the adsorption sites of the real composite.

This work was financially supported by the Russian Foundation for Basic Research (Project Nos 08-03-00824 and 10-03-00999) and the Council on Grants at the President of the Russian Federation (Program for State Support of the Leading Scientific Schools, Grant NSh-6512.2010.3).

References

1. G. C. Bond, C. L. Louis, D. T. Thompson, in *Catalysis by Gold*, Imperial College Press, London, 2007, 366 pp.
2. A. S. K. Hashmi, G. J. Hutchings, *Angew. Chem., Int. Ed. Engl.*, 2006, **45**, 7896.
3. H. Häkkinen, *Chem. Soc. Rev.*, 2008, **37**, 1847.
4. A. Deka, R. Deka, *J. Mol. Structure, THEOCHEM*, 2008, **870**, 83.
5. J. C. Fierro-Gonzaleza, B. C. Gates, *Chem. Soc. Rev.*, 2008, **37**, 2127.
6. S. M. Wetterer, D. J. Lavrich, T. Cummings, S. L. Bernasek, G. Scoles, *J. Phys. Chem. B*, 1998, **102**, 9266.
7. S. N. Lanin, D. A. Pichugina, A. F. Shestakov, V. V. Smirnov, S. A. Nikolaev, K. S. Lanina, A. Yu. Vasil´kov, Fam Tien Zung, A. V. Beletskaya, *Zh. Fiz. Khim.*, 2010, **84**, 2330 [*Russ. J. Phys. Chem.* (*Engl. Transl.*), 2010, **84**, 2133].
8. Kang Guo-Jun, Chen Zhao-Xu, Li Zhe, *J. Chem. Phys.*, 2009, **131**, 034710.
9. A. Lyalin, T. Taketsugu, *J. Phys. Chem. C*, 2010, **114**, 2484.
10. E. Bus, D. E. Ramaker, J. A. van Bokhoven, *J. Am. Chem. Soc.*, 2007, **129**, 8094.
11. S. Chretien, M. S. Gordon, H. Metiu, *J. Chem. Phys.*, 2004, **121**, 3756.
12. V. V. Smirnov, S. N. Lanin, A. Yu. Vasil´kov, S. A. Nikolaev, L. D. Murav´eva, E. V. Tyurina, E. V. Vlasenko, *Izv. Akad. Nauk, Ser. Khim.*, 2005, 2215 [*Russ. Chem. Bull., Int. Ed.*, 2005, **54**, 2286].
13. D. A. Pichugina, N. E. Kuz´menko, A. F. Shestakov, *Izv. Akad. Nauk, Ser. Khim.*, 2008, 1330 [*Russ. Chem. Bull., Int. Ed.*, 2008, **57**, 1356].
14. J. P. Perdew, K. Burke, M. Ernzerhof, *Phys. Rev. Lett.*, 1996, **77**, 3865.
15. D. A. Pichugina, A. F. Shestakov, N. E. Kuz´menko, *Zh. Fiz. Khim.*, 2004, **78**, 2027 [*Russ. J. Phys. Chem.* (*Engl. Transl.*), 2004, **78**, 1790].
16. D. A. Pichugina, A. F. Shestakov, N. E. Kuz´menko, *Gold Bull.*, 2007, **40**, 115.
17. Yu. A. Ustynyuk, D. N. Laikov, *Izv. Akad. Nauk, Ser. Khim.*, 2005, 804 [*Russ. Chem. Bull., Int. Ed.*, 2005, **54**, 820].
18. P. Pyykkö, *Chem. Soc. Rev.*, 2008, **37**, 1967.
19. W. J. Stevens, M. Krauss, H. Basch, P. G. Jasien, *Can. J. Chem.*, 1992, **70**, 612.
20. M. J. Frisch, G. W. Trucks, H. B. Schlegel, G. E. Scuseria, M. A. Robb, J. R. Cheeseman, J. A. Montgomery, Jr., T. Vreven, K. N. Kudin, J. C. Burant, J. M. Millam, S. S. Iyengar, J. Tomasi, V. Barone, B. Mennucci, M. Cossi, G. Scalmani, N. Rega, G. A. Petersson, H. Nakatsuji, M. Hada, M. Ehara, K. Toyota, R. Fukuda, J. Hasegawa, M. Ishida, T. Nakajima, Y. Honda, O. Kitao, H. Nakai, M. Klene, X. Li, J. E. Knox, H. P. Hratchian, J. B. Cross,

C. Adamo, J. Jaramillo, R. Gomperts, R. E. Stratmann, O. Yazyev, A. J. Austin, R. Cammi, C. Pomelli, J. W. Ochterski, P. Y. Ayala, K. Morokuma, G. A. Voth, P. Salvador, J. J. Dannenberg, V. G. Zakrzewski, S. Dapprich, A. D. Daniels, M. C. Strain, O. Farkas, D. K. Malick, A. D. Rabuck, K. Raghavachari, J. B. Foresman, J. V. Ortiz, Q. Cui, A. G. Baboul, S. Clifford, J. Cioslowski, B. B. Stefanov, G. Liu, A. Liashenko, P. Piskorz, I. Komaromi, R. L. Martin, D. J. Fox, T. Keith, M. A. Al-Laham, C. Y. Peng, A. Nanayakkara, M. Challacombe, P. M. W. Gill, B. Johnson, W. Chen, M. W. Wong, C. Gonzalez, J. A. Pople, *Gaussian 03*, *Rev. A.1*, Gaussian, Inc., Pittsburgh (PA), 2003.

21. S. A. Nikolaev, V. V. Smirnov, A. Yu. Vasil´kov, V. L. Podshibikhin, *Kinet. Katal.*, 2010, **51**, 396 [*Kinet. Catal.* (*Engl. Transl.*), 2010, **51**, 375].
22. A. Yu. Stakheev, L. M. Kustov, *Appl. Catal. A*, 1999, **188**, 3.
23. R. Meyer, C. Lemire, Sh. K. Shaikhutdinov, H.-J. Freund, *Gold Bull.*, 2004, **37**, 72.

Received July 2, 2010;
in revised form October 15, 2010